Effects of Magnetic Fields on Neutrino-dominated Accretion Model for Gamma-ray Bursts [*]

Yi Xie[1,2], Chang-Yin Huang[1] and Wei-Hua Lei[1]

[1] Department of Physics, Huazhong University of Science and Technology, Wuhan 430074
   sourcexieyi@gmail.com
[2] School of Physics and Information Engineering, Shanxi Normal University, Linfen 041004

Abstract Many models of gamma-ray bursts suggest a common central engine: a black hole of several solar masses accreting matter from a disk at an accretion rate from 0.01 to 10 $M_\odot$ s^{-1}, the inner region of the disk is cooled by neutrino emission and large amounts of its binding energy are liberated, which could trigger the fireball. We improve the neutrino-dominated accreting flows by including the effects of magnetic fields. We find that more than half of the liberated energy can be extracted directly by the large-scale magnetic fields in the disk, and it turns out that the temperature of the disk is a bit lower than the neutrino-dominated accreting flows without magnetic field. Therefore, the outflows are magnetically-dominated rather than neutrino dominated. In our model, the neutrino mechanism can fuel some GRBs (not the brightest ones), but cannot fuel X-ray flares. The magnetic processes (both BZ and electromagnetic luminosity from a disk) are viable mechanisms for most of GRBs and their following X-ray flares.

Key words: magnetic fields — accretion, accretion disks— neutrinos — gamma rays: bursts

1 INTRODUCTION

Gamma-ray bursts (GRBs) are flashes of gamma-rays occurring at cosmological distances, being the most powerful explosions since the Big Bang. They are generally divided into two classes (Kouveliotou et al. 1993): short-duration ($T_{90} < 2$s) hard-spectrum GRBs (SGRBs) and long-duration ($T_{90} > 2$s) soft-spectrum GRBs (LGRBs), being with different progenitors. LGRBs root in core collapses of massive, rapidly rotating stars (Woosley 1993; Paczynski 1998; Hjorth et al. 2003; Stanek et al. 2003), and supernovae have been observed coincidently in some LGRBs (Galama et al. 1998; Stanek et al. 2003; Hjorth 2003). In contrast to LGRBs, SGRBs may arise from coalescence of neutron stars or black hole binary systems due to damping of gravitational radiation (e.g. Eichler et al. 1989; Narayan, Paczynski & Piran 1992; Fryer & Woosley 1998), and they are probably associated with elliptical galaxies (Gehrels et al. 2005; Bloom et al. 2006; Barthelmy et al. 2005; Berger et al. 2005). It is believed that the two processes give rise to a black hole of several solar masses with a magnetized disk or a torus around it (Meszaros & Rees 1997b). Many central engine models of GRBs are built based on this scenario (exceptions are, for instance, magnetized rotating neutron stars, see Usov 1992).

Some authors have studied the accretion model for GRBs assuming steady-state accretion (e.g. Papham, Woosley & Fryer 1999, hereafter PWF; Narayan, Piran & Kumar 2001, hereafter NPK; Di Matteo, Perna & Narayan 2002, hereafter DPN). Their studies show that at the extremely high accretion rate (0.01 to 10 $M_\odot$ s^{-1}) needed to power GRBs, the disk cannot be cooled efficiently as the gas photon opacities are

very high, and a large fraction of its energy is advection dominated. However, the inner region of the disk becomes hot and dense enough to cool via neutrino emission, and this accretion mode is referred to as neutrino-dominated accretion flows (NDAFs). The neutrinos can liberate large amounts of binding energy via the $\nu\bar{\nu} \to e^+e^-$ processes in regions of low baryon density and then trigger the fireball.

The model with "neutrino-driven outflow" alone, however, cannot be a candidate for some GRBs central engines. For instance, numerical simulations by Shibata et al. (2006) suggested that the collapse of hypermassive neutron-star triggered by gravitational wave cannot be a candidate for the central engine of SGRBs, but it becomes powerful enough to produce the fireball after taking the magnetic braking and magneto-rotational instability (MRI, Balbus & Hawley 1991) into account. On the other hand, researches showed that the magnetic fields can be magnified up to $10^{15} \sim 10^{16}$ G by virtue of MRI or dynamo processes (Pudritz & Fahlman 1982 and references therein) in the inner region of the disk. So, the existence of strong magnetic fields should be considered. Both PWF and DPN compared the luminosity of neutrino emission and the Poynting flux, and indicated that MHD processes are viable mechanisms for powering GRBs, but these authors did not include magnetic fields in their disk conditions. Some authors have studied the analytic model of GRBs that a black hole with a magnetized thin disk around it (e.g. Wang et al. 2002, 2006), however, they never discussed the processes of neutrino emission.

Here we intend to improve the NDAFs model by considering the effects of magnetic braking and magnetic viscosity. The equation of angular momentum of a standard disk is replaced by the equation of a magnetized disk in which viscosity is caused by magnetic braking and is magnetic viscosity only. We then deduce the rotational energy extracted by the large-scale fields in the disk from the thermal energy produced by viscous dissipation, and the magnetic pressure is considered in the equation of state. It turns out that the inner region of the disk is magnetically dominated. Magnetized accretion models in the GRB context have also been discussed in several other papers that included detailed numerical simulations. For example, Proga et al. (2003) studied an MHD collapsar accretion model and suggested that MHD effects alone can launch a GRB jet, which is Poynting flux dominated. Mizuno et al. (2004a,b) drew similar conclusions using a GR-MHD code. These results agree with the conclusions of this paper.

This paper is organized as follows. In Section 2 we outline the theory of magnetized accretion disk. In Section 3 we introduce the basic assumptions and equations of our model. In Section 4 we show the numerical results of our model, and finally, Section 5 summarizes the main results of our model and some defects of it are also discussed.

2 DESCRIPTION OF A MAGNETIZED ACCRETION DISK

It is widely known that the magnetic fields on an accretion disk can greatly affect the angular momentum transfer and hence the accretion rate via a variety of modes. In this paper we only consider two basic mechanisms: the first one is magnetic viscosity, the weak magnetic fields create MRI in which turbulence dominates the angular momentum transfer (Balbus & Hawley 1991). The second is magnetic braking: the large scale magnetic field extracts rotational energy of the disk due to the shear force of differential rotation (Blandford 1976; Blandford & Payne 1982; Livio et al. 1999). We assume that the accretion process is governed by these two mechanisms completely. The main points of the magnetized accretion disk model (in which the magnetic braking and magnetic viscosity are considered only for the angular momentum transfer) given by Lee et al. (2000) are outlined as follows.

According to Torkelsson et al. (1996) the magnetic viscosity ν^{mag} is defined as

$$B_\phi B_r/4\pi = -\nu^{\mathrm{mag}} \left(rd\Omega_{\mathrm{disk}}/dr\right)\rho\,, \tag{1}$$

where B_ϕ and B_r are respectively the azimuthal and radial component fields, Ω_{disk} is the angular velocity and ρ is the density of the disk matter. The magnetic viscosity ν^{mag} can be parameterized as (Shakura & Sunyaev 1973; Pringle 1981),

$$\nu^{\mathrm{mag}} = \alpha^{\mathrm{mag}} c_{\mathrm{s}} H\,, \tag{2}$$

where c_{s} is the sound velocity of the disk ($c_{\mathrm{s}} = \left(P_{\mathrm{disk}}/\rho\right)^{1/2}$, in which P_{disk} is the disk pressure) and H is the half-thickness of the disk. Invoking hydrostatic equilibrium perpendicular to the disk plane, we have $H = c_{\mathrm{s}}/\Omega_{\mathrm{disk}}$ and

$$\nu^{\mathrm{mag}} = \alpha^{\mathrm{mag}} c_{\mathrm{s}}^2/\Omega_{\mathrm{disk}}\,. \tag{3}$$

For a Keplerian orbit we have $\Omega_{\mathrm{disk}} \sim \Omega_{\mathrm{K}} = \left(GM/r^3\right)^{1/2}$, and Equation (1) can be written as

$$B_\phi B_r / 4\pi = \frac{3}{2} \alpha^{\mathrm{mag}} P_{\mathrm{disk}} . \tag{4}$$

The accretion rate is generally determined by the magnetic braking for $H \ll r$ (Lee, Wijers & Brown 2000), and the angular momentum balance equation can be written as

$$\dot{M} = 2r B_\phi B_Z / \Omega_{\mathrm{disk}}. \tag{5}$$

The axisymmetric solution (Blandford 1976) is

$$B_\phi = 2r \Omega_{\mathrm{disk}} B_Z / c. \tag{6}$$

A roughly steady state will be reached when the growth rate of B_ϕ generated by differential rotation from the radial field equals to its loss rate by buoyancy, then the magnitude of B_ϕ can be estimated as (Katz 1997)

$$B_\phi \approx \left[\frac{3}{2} B_r \Omega_{\mathrm{disk}} H \right]^{1/2} (4\pi\rho)^{1/4} . \tag{7}$$

From Equations (4), (6) and (7) we have

$$B_Z = \frac{c}{2} \left(\frac{\pi r P_{\mathrm{disk}}}{GM} \right)^{1/2} (9\alpha^{\mathrm{mag}})^{1/3} , \tag{8}$$

and

$$B_\phi = (\pi P_{\mathrm{disk}})^{1/2} (9\alpha^{\mathrm{mag}})^{1/3} . \tag{9}$$

The vertical component and azimuthal component of field can be estimated from Equations (8) and (9), and for a given α^{mag}, they only depend on the gas pressure.

Combining Equations (6) and (8) with Equation (5) we have (see also Lee, Wijers & Brown 2000)

$$\dot{M} = 4r^2 B_Z^2 / c. \tag{10}$$

Since $\dot{M}$ is independent of r in steady-state accretion, we can infer that $B_Z \propto 1/r$.

3 BASIC ASSUMPTIONS AND EQUATIONS OF MODEL

The basic physical conditions in disk models for GRBs can be derived by virtue of the steady-state conditions (PWF, NPK, DPN). Based on these studies, we consider the effects of magnetic field in the inner regions of the disks in the frame of hydrodynamics. The basic equations consist of the equation of state and the conservation equations of energy and angular momentum in a magnetized accretion disk. These are described as follows.

In the equation of state we include the contributions from radiation pressure, gas pressure, degeneracy pressure and magnetic pressure,

$$P = \frac{11}{12} aT^4 + \frac{\rho k T}{m_p} + \frac{2\pi hc}{3} \left(\frac{3}{8\pi m_p} \right)^{4/3} \left(\frac{\rho}{\mu_e} \right)^{4/3} + \frac{B^2}{8\pi}, \tag{11}$$

where a is the radiation constant, T is the disk temperature, and the factor $\frac{11}{12}$ includes the contribution of relativistic electron-positron pairs. In the degeneracy term, μ_e is the mass per electron, and it is taken as 2 by assuming equal number of protons and neutrons. For the magnetic pressure we only consider the poloidal component in the calculation, provided that it is not much less than the toroidal component.

The conservation of mass is written by NPK and DPN as

$$\dot{M} = 4\pi r \upsilon_{\mathrm{r}} \rho H \approx 6\pi \rho \nu H, \tag{12}$$

where υ_{r} is the radial velocity and $\upsilon_{\mathrm{r}} = 3\nu/2r$. Different from NPK and DPN, we replace Equation (12) by Equation (10), which includes the effects of magnetic braking and magnetic viscosity.

In the energy equation, the viscous heating equals the neutrino radiative loss plus advective loss and the fraction of rotational energy extracted by large-scale magnetic fields,

$$\frac{3GM\dot{M}}{8\pi r^3} = \left(q_{\nu\bar{\nu}}^- + q_{eN}^-\right) H + q_{\mathrm{adv}} + Q_B^-, \tag{13}$$

in which $q_{\nu\bar{\nu}}^-$ is cooling via pair annihilation and we take it in the approximation of Itoh et al. (1989, 1990): $q_{\nu\bar{\nu}}^- \simeq 5 \times 10^{33} T_{11}^9$ erg cm^{-3} s^{-1} (in which $X_n = X/10^n$ is used), q_{eN}^- represents the cooling via pair capture on the nuclei, and can be estimated as $q_{eN}^- \simeq 9 \times 10^{33} \rho_{10} T_{11}^6$ erg cm^{-3} s^{-1}. We approximate the advective cooling rate q_{adv} by (see e.g., Narayan & Yi 1994; Abramowicz et al. 1995)

$$q_{\mathrm{adv}} = \Sigma \nu T \frac{ds}{dr} \simeq \xi \nu \frac{H}{r} T \left(\frac{11}{3} a T^3 + \frac{3}{2} \frac{\rho k T}{m_p} \frac{1 + X_{\mathrm{nuc}}}{4}\right), \tag{14}$$

in which s is the specific entropy, X_{nuc} is the mass fraction of free nucleons, $\xi \propto -d\ln s/d\ln r$ is assumed to be equal to 1 as in DPN, and Q_B^- represents the energy extracted by the magnetic field (Lee, Wijers & Brown 2000)

$$Q_B^- = \frac{dP^{\mathrm{mag}}}{dS} = \frac{B_Z^2 r^2}{\pi c} \left(\frac{GM}{r^3}\right) = \frac{GM\dot{M}}{4\pi r^3}, \tag{15}$$

where $dS = 2\pi r dr$. Comparing Equation (15) with Equation (13), we find that two thirds of the energy of viscous heating was extracted by the field, thus, it is magnetically dominated in the inner region of the disk.

Equations (8), (10), (11) and (13) contain four independent unknowns P, ρ, T and B_Z as functions of r and constitute a complete set of equations which can be numerically solved with given M, α (for simplicity, we omit the superscript 'mag') and $\dot{M}$. In the following calculations we fix $M = 3M_\odot$ (the corresponding Schwarzschild radius R_S is $2GM/c^2 = 8.85 \times 10^5$ cm), and $\alpha = 0.1$.

4 NUMERICAL RESULTS

4.1 Gas Profiles

We show the numerical solutions of the full equations in this section, obtained with by numerical algorithm with the Newton iteration method given in the software of "Mathematica". The pressure components profiles are shown in Figure 1, panels (a), (b) and (c) show respectively the solutions for three values of the accretion rate $\dot{m} = 0.1, 1$ and 10 ($\dot{m}$ is defined as $\dot{m} = \dot{M}/M_\odot$ s^{-1}). The gas pressure, degeneracy pressure, radiation pressure, and magnetic pressure are shown by the solid line, dotted line, dashed line and long-dashed line in each panel. From Figure 1 we obtain the following results:

(i) From (a) we can see that the flow is radiation pressure dominated in the region $1R_S \sim 10R_S$ and may be thermally unstable (see Sect. 4.3, stability analysis). It is thermally stable in the same region in DPN where the flow is always dominated by gas pressure.

(ii) From (b) and (c) we can see that, the magnetic pressure component is more important at large radii and even overwhelms the gas pressure and degeneracy pressure. So our model is valid only in a narrow region because of the restriction of Equation (12).

Figure 2 shows the temperature profiles (panel a) and density profile (b) calculated from our model for three values of the accretion rate, $\dot{m} = 0.1$ (long-dashed line), 1 (dashed line) and 10 (short-dashed line). Compared to DPN (see DPN, fig. 1), we find that the temperature of the disk is a little lower than in NDAFs without considering the effects of magnetic fields, and the density drops much more rapidly with the radius.

4.2 BZ Luminosity, Electromagnetic Luminosity from Disk, and Neutrino Luminosity

It is a common assumption that the magnetic fields will rise up to some fraction of its equipartition value, $B^2/8\pi \sim \rho c_s^2$ (for instance, 10% in DPN). For $0.1 < \dot{m} < 10$, typical values of ρc_s^2 are $10^{30} \sim 10^{32}$ erg cm^{-3}, corresponding to field strengths of $10^{15} \sim 10^{16}$ G. The BZ jet luminosity is then

$$L_{\mathrm{BZ}} = \frac{B_H^2}{4\pi} \pi c a^2 R_S^2 \simeq 10^{52} a^2 \left(\frac{B_H}{10^{16}\mathrm{G}}\right)^2 \left(\frac{M}{3M_\odot}\right)^2 \mathrm{erg\ cm}^{-3}, \tag{16}$$
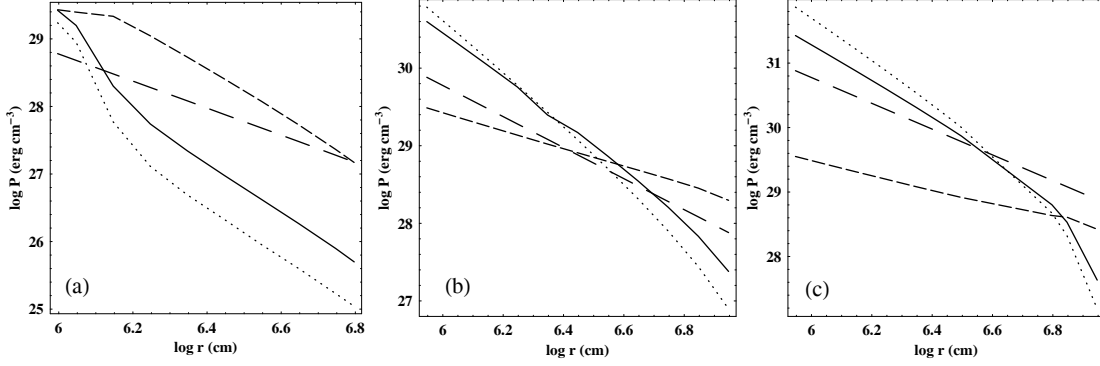
Fig. 1 Profiles of pressure components for three values of the accretion rate: (a) $\dot{m} = 0.1$, (b) $\dot{m} = 1$, and (c) $\dot{m} = 10$. The gas pressure is shown by the solid line, the degeneracy pressure by the dotted line, the radiation pressure by the dashed line, and magnetic pressure by the long-dashed line.
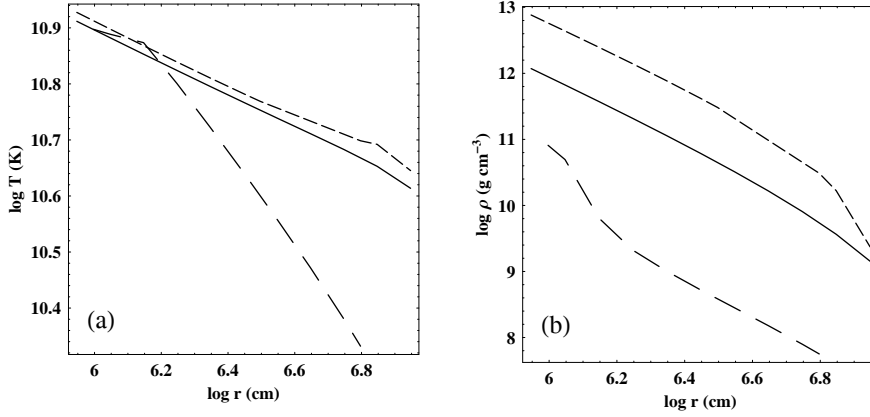

Fig. 2 Panel (a) shows the temperature profiles and panel (b), the density profiles, for three values of the accretion rate: $\dot{m} = 0.1$ (long dashed line), $\dot{m} = 1$ (solid line) and $\dot{m} = 10$ (short dashed line).

in which a is the dimensionless black hole spin parameter, B_H is the magnetic field at the horizon.

The electromagnetic power output from a disk is equal to the power of the disk magnetic braking and can be calculated as (Livio et al.1999; Lee et al. 2000)

$$L_d = \frac{B_z^2}{4\pi}\pi r^2 \left(\frac{r\Omega_{\mathrm{disk}}}{c} \right) c \approx a^{-2} \left(\frac{B_Z}{B_\mathrm{H}} \right)^2 \left(\frac{r}{R_\mathrm{S}} \right)^{3/2} L_{\mathrm{BZ}}. \tag{17}$$

Consistent with previous work (Merloni & Fabian 2002; DPN), we take approximately,

$$B_Z \sim (H/r)\, B_\mathrm{H}. \tag{18}$$

It is easy to obtain the strength of the poloidal field in the disk and the field at the black hole horizon for a given $\dot{m}$ by using Equations (10) and (18) in our model, without the assumption of the equipartition value discussed above, and then the BZ jet luminosity and electromagnetic power from a disk can be calculated from Equations (16) and (17). The neutrino luminosity is given by $L_\nu = \int_{r_{\min}}^{r_{\max}} 2\pi q_\nu^- r\, dr$, in which $q_\nu^- = \left(q_{\nu\bar\nu}^- + q_{eN}^- \right) H$, $r_{\min} = 1 R_\mathrm{S}$ (for an extreme Kerr black hole), and $r_{\max} = 10 R_\mathrm{S}$. We estimate the luminosity due to $\nu\bar\nu$ annihilation along the z-axis above the disk from Equation (21) in DPN.

In Figure 3 we show the curves of BZ luminosity $L_{\rm BZ}$ (solid lines), electromagnetic luminosity from a disk L_d (long-dashed line), and neutrino annihilation luminosity $L_{\nu\bar{\nu}}$ (short-dashed line) versus dimensionless accretion rate. From Figure 3, we obtain the following results:

(i) L_d is larger than $L_{\rm BZ}$ for $H/r = 0.2$ (solution of this model). However, both of them are viable mechanisms for the central engine of GRBs, and can also fuel the observed X-ray flares, in which case the accretion rate of $\dot{m} = 0.01$ is needed.

(ii) $L_{\nu\bar{\nu}}$ is around 10^{51} erg s^{-1} at $\dot{m} = 1$, which is sufficient to power some GRBs. At the accretion rate of $\dot{m} = 0.01$, it fails to fuel the X-ray flares.
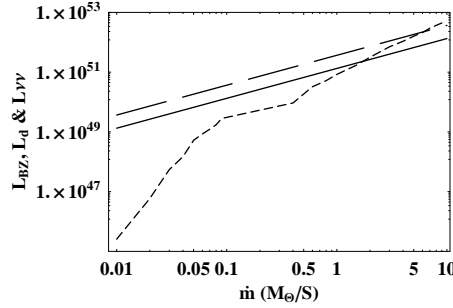

Fig. 3 Solid line represents the BZ luminosity, long-dashed line, the electromagnetic luminosity from the disk and short-dashed line, the neutrino annihilation luminosity as a function of the accretion rate, for $H/r = 0.2$.

In conclusion, the neutrino mechanism can fuel some GRBs (not the brightest ones), but cannot fuel X-ray flares. However, the magnetic processes (both BZ and electromagnetic luminosity from a disk) are viable mechanisms for most of the GRBs and their following X-ray flares (this agrees well with the discussion of Fan et al. 2005).

4.3 Stability

Both NPK and DPN discussed the stability properties of their solutions. Since our model considers the effects of magnetic fields and differs considerably with theirs, it is interesting to examine whether our solution is stable.

The general condition for thermal stability is given by (Piran 1978)

$$\left(\frac{d\ln Q^+}{d\ln T}\right)_{|\Sigma} < \left(\frac{d\ln Q^-}{d\ln T}\right)_{|\Sigma}, \tag{19}$$

in which $Q^{\pm}$ are the integrated (over the height of the disk) heating (+) and cooling (−) rates. The cooling rate is $Q^- = q_\nu^- + q_{\rm adv} + Q_B^-$. We show the two curves of Q^- and Q^+ as functions of the gas temperature in Figure 4. The radius is fixed at $r = 5R_{\rm S}$, while the surface density is taken to be $\Sigma = 10^{16}$ g cm^{-2}. From Figure 4 we can see that, the flow is unstable while the temperature T is below 5×10^{10} K, because that the magnetic field's extraction of rotational energy from the disk is independent of the temperature. When $T > 5 \times 10^{10}$ K, the flow becomes stable because $q_{eN}^- \propto T^6$ becomes relatively more significant as the temperature increases. When the disk temperature crosses the critical point for instability, the thermal energy would be released suddenly in a thermal time scale. It is a possible explanation for the variability on time scales of tens of ms in the GRB light curves, and we will give the details in another paper.

Following NPK and DPN we use the condition for viscous stability
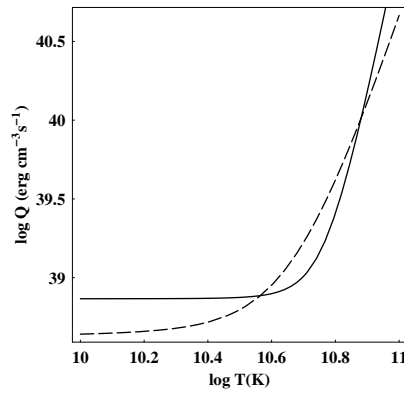
$$\frac{d\dot{M}}{d\Sigma} > 0 \,. \tag{20}$$

Fig. 4 Thermal stability analysis. Dashed line shows Q^+, and solid line shows Q^-, as functions of T for $r = 5R_S$ curves, and for $\Sigma = 10^{16}$ g cm^{-2}. The solution is unstable while $T < 5 \times 10^{10}$ K, and becomes stable when $T > 5 \times 10^{10}$ K.

In our model, we have $\dot{M} \propto \Sigma$ for the gas pressure domination case, $\dot{M} \propto \Sigma^{8/7}$ in the degeneracy pressure case, and $\dot{M} \propto \Sigma^2$ in the radiation pressure case, and we have $\dot{M} \propto B^2 \propto P$ for the magnetic pressure dominated case, and the surface density $\Sigma \propto P^{1/2}\rho^{1/2}$. Meanwhile, considering that the magnetic field decreases as r^{-1}, we have approximately $\rho \propto r^{-3}$, and then $\dot{M} \propto \Sigma$. Clearly, all these cases are viscously stable.

Finally, we also considered gravitational instability. The accretion flow will become gravitationally unstable if the Toomre parameter Q_T is less than 1. For a Keplerian orbit, Q_T is given by (Toomre 1964)

$$Q_T = \frac{c_s \kappa}{\pi G \Sigma} = \frac{\Omega_K^2}{\pi G \rho}.$$
(21)

We have checked that $Q_T \gg 1$ hence the flow is gravitationally stable in the inner region of the disk. Nevertheless, at large radii the Toomre parameter could be less than 1 as argued by Perna et al. (2006), but actually that was for another model for X-ray flares.

5 CONCLUSIONS AND DISCUSSION

In this paper we modify the NDAFs model as a central engine for GRB by considering the effects of magnetic braking and magnetic viscosity in the frame of Newtonian dynamics. We found that two thirds of the liberating energy was extracted directly by the large-scale magnetic field in the disk and that the disk temperature is a bit lower than in the NDAFs model without magnetic fields. Furthermore, the disk density falls faster along the radius than in NDAFs. Therefore, the inner region of the flow is magnetically dominated rather than neutrino dominated. However, the neutrino mechanism can still fuel some GRBs (not the brightest ones), but cannot fuel X-ray flares. The magnetic processes (both BZ and electromagnetic luminosity from a disk) are viable mechanisms for most of GRBs and their following X-ray flares.

Our model is formulated invoking Newtonian potential and ignoring the effects of general relativity, which may be important in some aspects (Gu et al. 2006), and neutrino opacity. In particular, underlying the main simplification of the present analytic approach is the requirement of a steady state, which may not necessarily be justified in reality or numerical simulations. For example, when magnetic fields are included, both numerical simulations (Proga & Begelman 2003) and analytical arguments (Proga & Zhang 2006) suggested that the accretion flow may not always in a steady state. Rather, magnetic fields accumulated near the black hole can form a magnetic barrier that temporarily blocks the accretion flow. This creates some dormant epochs at the central engine. Breaking of the barrier would lead to a restarting of the central engine, which could explain the recent Swift observations of X-ray flares (for a review of the Swift results and, in particular, the X-ray flares and their interpretations, see Zhang 2007). In this paper, the poloidal component of magnetic fields is $B_Z \propto 1/r$, which implies that the magnetic pressure drops much more

slowly than the other components and the calculations indicate that the magnetic field pressure could be dominant at larger radii. In fact, such over-pressure magnetic fields are the agent to form the magnetic barrier as reported by Proga & Zhang (2006), which is needed to interpret the observed X-ray flares. The unsteady state accretion model and the case of over-pressure magnetic fields will be studied in our future work.

References

Abramowicz M. A., Chen X., Kato S., Lasoto J. P., Regev O., 1995, ApJ, 438, L37
Balbus S. A., Hawley J. F., 1991, ApJ, 376, 214
Berger E. et al., 2005, Nature, 438, 988
Barthelmy S. D. et al., 2005, Nature, 438, 994
Blandford R. D., 1976, MNRAS, 176, 456
Blandford R. D., Payne D. G., 1982, MNRAS, 199, 883
Blandford R. D., Znajek R. L., 1977, MNRAS, 179, 433
Bloom J. S. et al., 2006, ApJ, 638, 354
Eichler D., Livio M., Piran T., Schramm D. N., 1989, Nature, 340, 126
Fan Y. Z., Zhang B., Proga D., 2005, ApJ, 635, L129
Fryer C. L., Woosley S. E., 1998, ApJ, 502, L9
Galama T. J., 1998, Nature, 395, 670
Gehrels N. et al., 2005, Nature, 437,851
Ghosh P., Abramowicz M. A., 1997, MNRAS, 292, 887
Gu W. M., Liu T., Lu J. F., 2006, ApJ, 643, L87
Hjorth J. et al., 2003, Nature, 423, 847
Lee H. K., Wijers R. A. M. J., Brown G. E., 2000, PhR, 325, 83
Livio M., Ogilvie G. I., Pringle J. E., 1999, ApJ, 512, 100
Katz J. I., 1997, ApJ, 490, 633
Kouveliotou C. et al., 1993, ApJ, 413, L101
Narayan R., Piran T., Kumar P., 2001, ApJ, 557, 949 (NPK)
Narayan R., Paczynski B., Piran T., 1992, ApJ, 395, L83
Narayan R., Yi I., 1994, ApJ, 428, L13
Di Matteo T., Perna R., Narayan R., 2002, ApJ, 579, 706 (DPN)
Mizuno Y. et al., 2004a, ApJ, 606, 395; 2004b, ApJ, 615, 389
Merloni A., Fabian A. C., 2002, MNRAS, 332, 165
Meszaros P., Rees M. J., 1997, ApJ, 482, L29
Paczynski B., 1998, ApJ, 494, L45
Perna R., Armitage P., Zhang B., 2006, ApJ, 636, L29
Proga D. et al., 2003, ApJ, 599, L5
Proga D., Begelman M. C., 2003, ApJ, 592, 767
Proga D., Zhang B., 2006, MNRAS, 370, L61
Popham R., Woosley S. E., Fryer C., 1999, ApJ, 518, 356 (PWF)
Prian T., 1978, ApJ, 221, 652
Pringle J. E., 1981, ARA&A, 19, 137
Pudritz R. E., Fahlman G. G., 1982, MNRAS, 198, 689
Shakura N. I., Sunyaev R. A., 1973, A&A, 24, 337
Shibata M. et al., 2006, PRL , 96, 031102
Stanek K. Z. et al., 2003, ApJ, 591, L17
Toomre A., 1964, ApJ, 139, 1217
Torkelsson U., Brandenburg A., Nordlund A. et al., 1996, Astrophys. Lett. Comm., 34, 383
Usov V. V., 1992, Nature, 357, 472
Wang D. X., Lei W. H., Xiao K. et al., 2002, ApJ, 580, 358
Wang D. X., Lei W. H., Ye Y. C. et al., 2006, ApJ, 643, 1047
Woosley S. E., 1993, ApJ, 405, 273
Zhang B., 2007, Chin. J. Astron. Astrophys. (ChJAA), 7, 1